



*Supplement of*

## **Changing sources and burial of organic carbon in the Chukchi Sea sediments with retreating sea ice over recent centuries**

**Liang Su et al.**

*Correspondence to:* Jian Ren ([jian.ren@sio.org.cn](mailto:jian.ren@sio.org.cn)) and Jianfang Chen ([jfchen@sio.org.cn](mailto:jfchen@sio.org.cn))

The copyright of individual parts of the supplement might differ from the article licence.

## Supplementary Figures

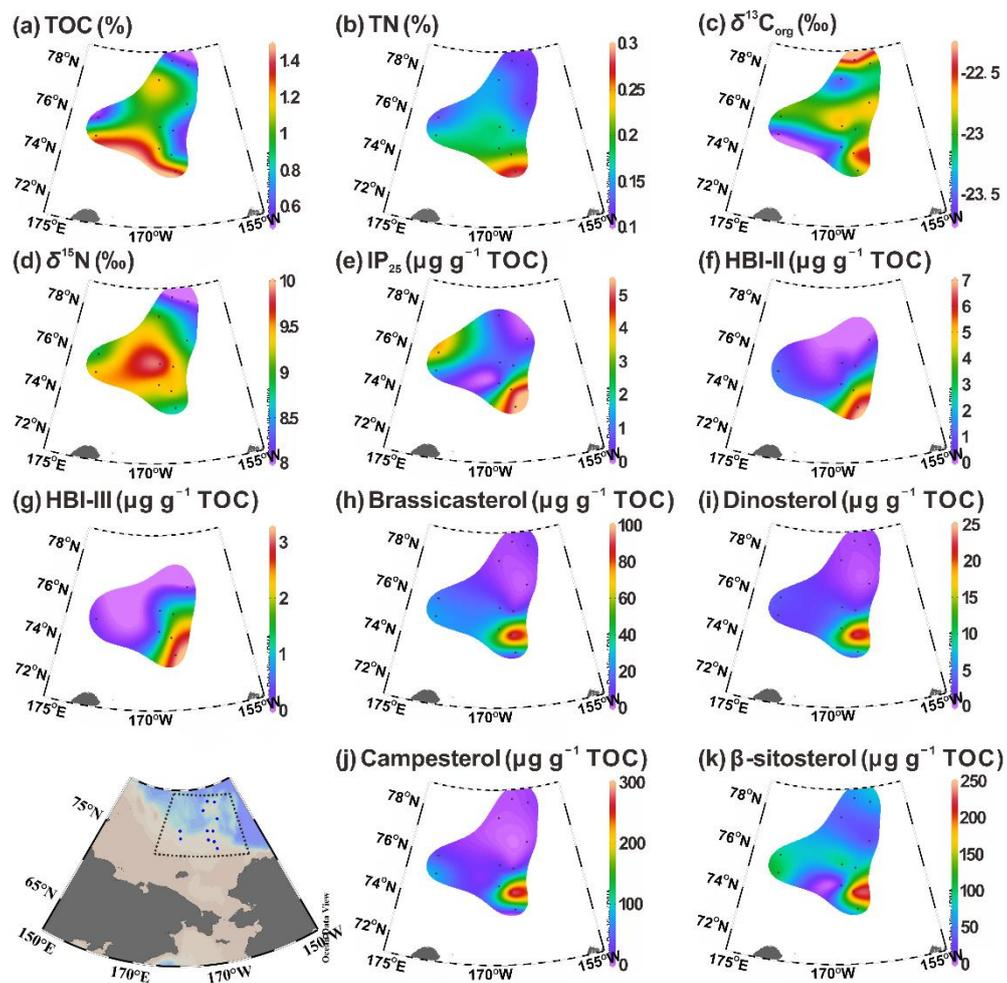


**Figure S1.** Distribution of (a) TOC, (b) TN, (c)  $\delta^{13}\text{C}_{\text{org}}$ , (d)  $\delta^{15}\text{N}$ , (e)  $\text{IP}_{25}$ , (f) HBI-II, (g) HBI-III, (h) brassicasterol, (i) dinosterol, (j) campesterol and (k)  $\beta$ -sitosterol in the surface sediments of Chukchi Sea and Chukchi Plateau.

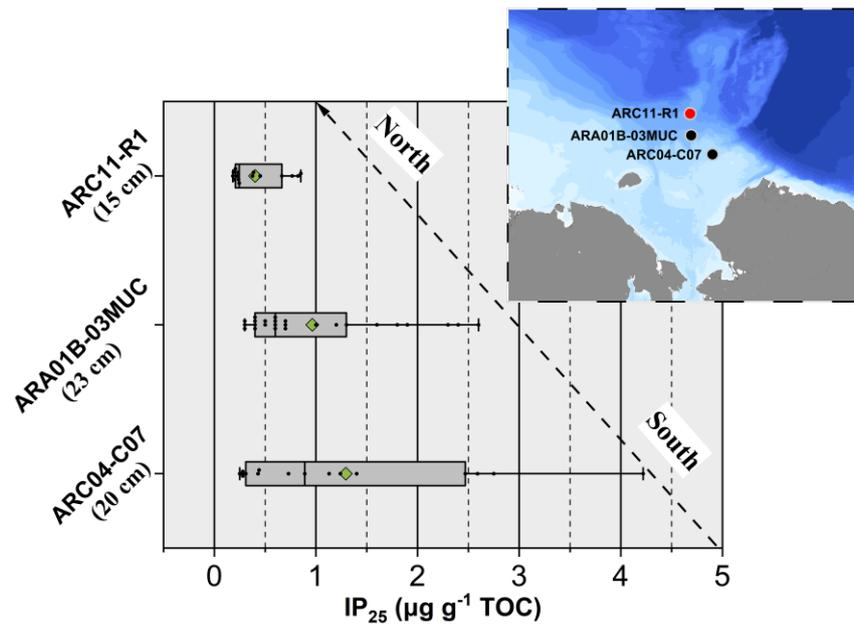


**Figure S2.** Box plot of IP<sub>25</sub> concentrations in 3 sediment cores (ARC04-C07, Bai et al. (2022); ARA01B-03MUC, Kim et al. (2019); ARC11-R1, this study). The map in the upper right shows their locations. The central bar in the boxes represents the median value and the green diamond represents the mean value. The rightmost and leftmost of the boxes represent the 75th and 25th percentiles, respectively. Whiskers are the maximum and minimum values within 1.5 times the interquartile range.

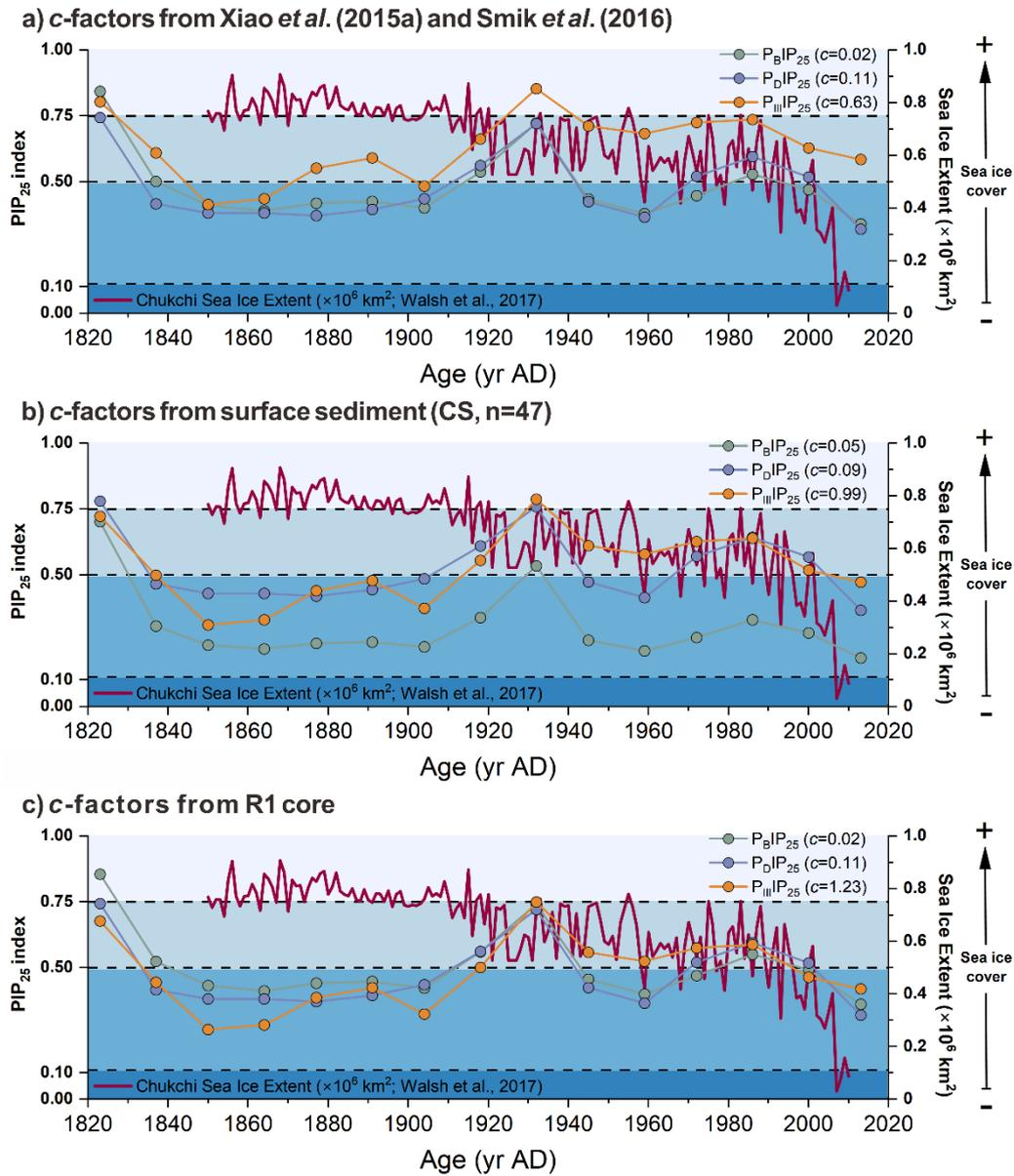


**Figure S3.** PIP<sub>25</sub> values calculated from different database *c*-factors from: (a) Xiao *et al.* (2015a) and Smik *et al.* (2016); (b) surface sediments from the Chukchi Sea in this study; (c) from R1 core.

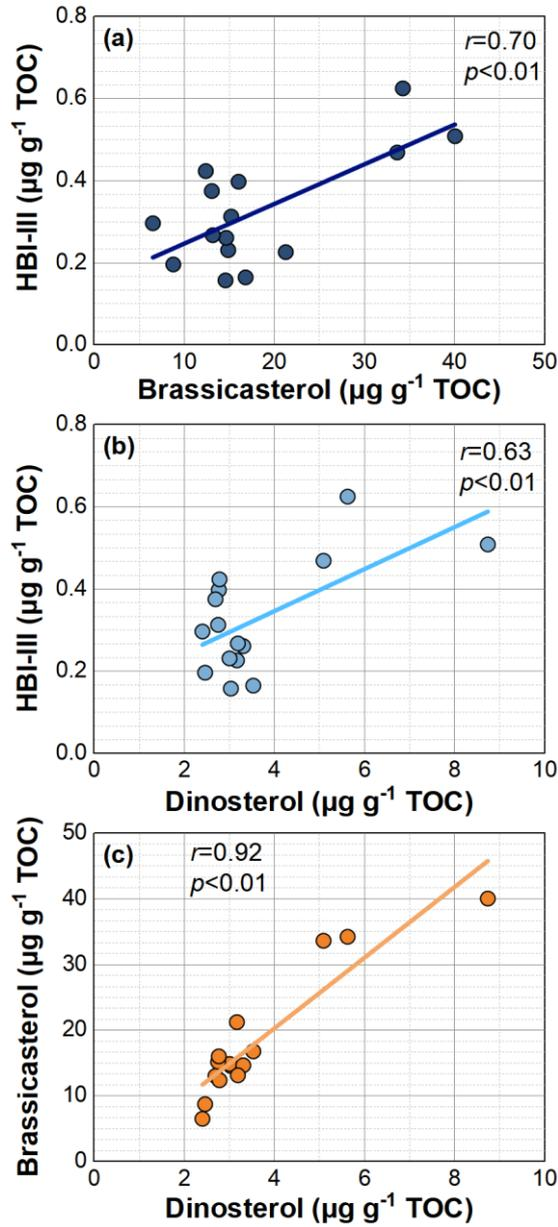


**Figure S4.** (a) Correlation between brassicasterol concentrations and HBI-III concentrations. (b) Correlation between dinosterol concentrations and HBI-III concentrations. (c) Correlation between dinosterol concentrations and brassicasterol concentrations calculated along core R1.

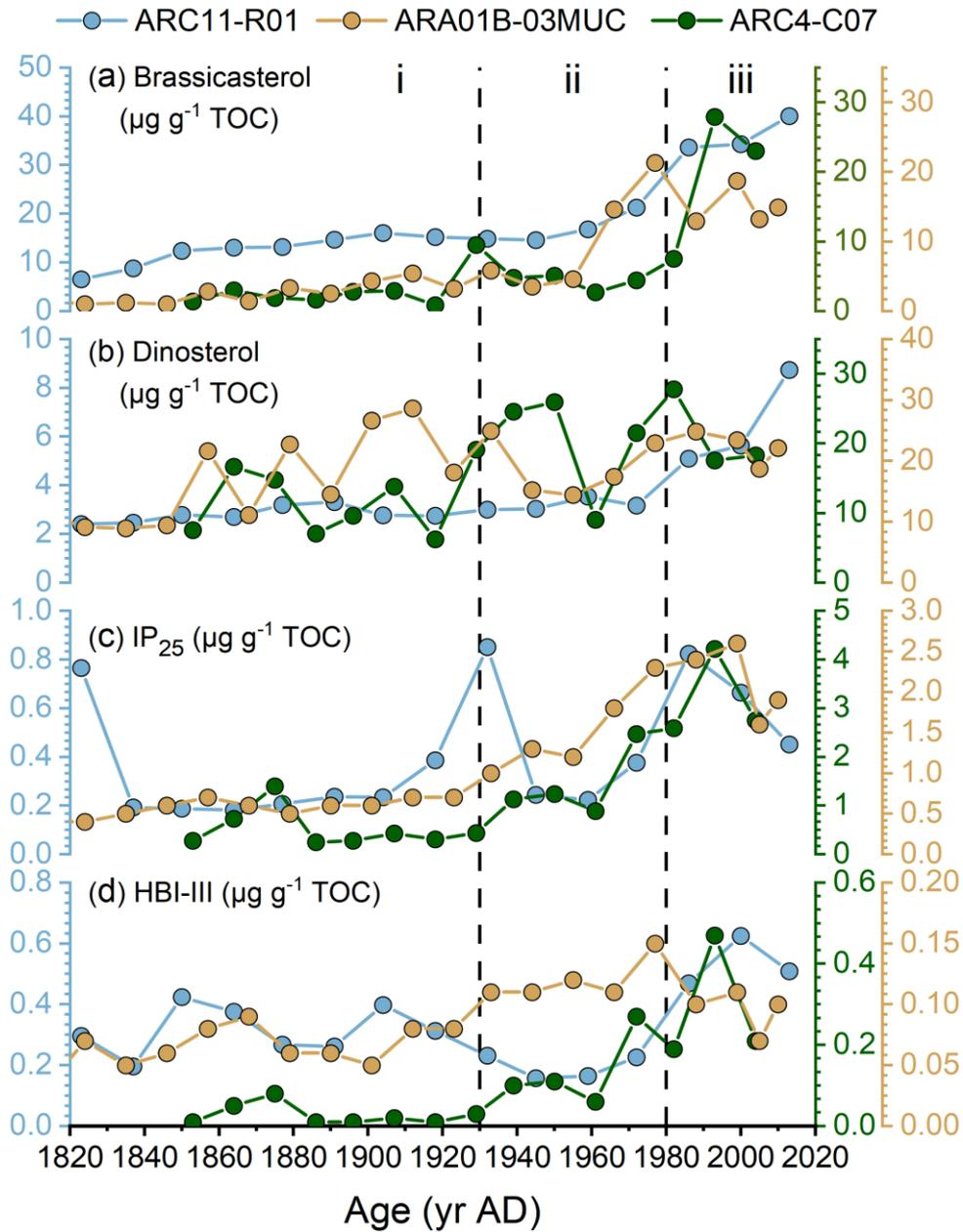


**Figure S5.** Downcore biomarker profiles of (a) brassicasterol concentration, (b) dinosterol concentration, (c)  $\text{IP}_{25}$  concentration and (d) HBI-III concentration in the core ARC04-C07 (Bai et al. 2022), ARA01B-03MUC (Kim et al. 2019) and ARC11-R1.

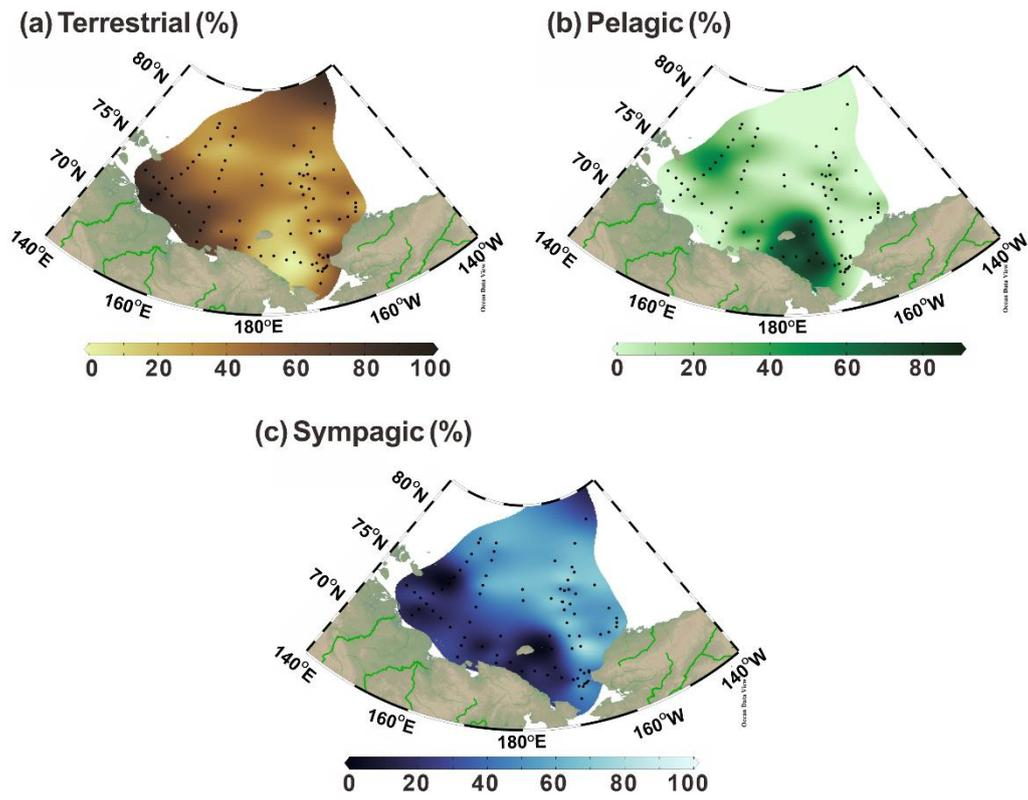


**Figure S6.** Proportion of organic carbon from each source in surface sediment: (a) terrestrial, (b) pelagic, and (c) sympagic.

## Supplementary Table

**Table S1.** Summary of TOC, H-Print,  $\delta^{13}\text{C}_{\text{org}}$  and proportion of overall organic carbon from each source ( $f_{\text{oc}}$  (%), based on  $\delta^{13}\text{C}_{\text{org}}$  and H-Print, and OC ( $\text{mg g}^{-1}$  d. w., dry weight)) data from surface sediment across the East Siberian Sea and the Chukchi Sea.

Cruise	Station	Longitude	Latitude	TOC (%)	H-Print (%)	$\delta^{13}\text{C}_{\text{org}}$ (‰)	$f_{\text{sym}}$ (%)	$f_{\text{pela}}$ (%)	$f_{\text{terr}}$ (%)	OC <sub>sym</sub> ( $\text{mg g}^{-1}$ d. w.)	OC <sub>pela</sub> ( $\text{mg g}^{-1}$ d. w.)	OC <sub>terr</sub> ( $\text{mg g}^{-1}$ d. w.)
LV77	LV77-2	-169.91	68.58	1.25	78.18	-23.75	8.95	78.18	12.87	1.12	9.78	1.61
LV77	LV77-3	-172.15	68.88	2.06	80.69	-23.19	15.46	80.69	3.85	3.18	16.58	0.79
LV77	LV77-4	-174.90	69.20	2.01	81.28	-22.97	18.33	81.28	0.39	3.68	16.33	0.08
LV77	LV77-5	-173.21	69.71	1.69	81.57	-23.34	12.82	81.57	5.61	2.17	13.79	0.95
LV77	LV77-6	-173.61	72.20	1.78	70.79	-23.58	15.55	70.79	13.66	2.76	12.58	2.43
LV77	LV77-7	-173.49	71.18	0.86	76.46	-24.05	5.58	76.46	17.96	0.48	6.59	1.55
LV77	LV77-8	-177.48	69.59	0.95	57.98	-23.48	24.27	57.98	17.75	2.31	5.52	1.69
LV77	LV77-9	179.86	69.59	0.60	77.77	-23.80	8.45	77.77	13.78	0.51	4.66	0.83
LV77	LV77-10	177.31	70.25	1.32	63.42	-24.04	13.15	63.42	23.43	1.73	8.34	3.08
LV77	LV77-11	174.34	70.12	1.06	18.93	-25.19	22.14	18.93	58.93	2.35	2.01	6.26
LV77	LV77-12	174.36	70.73	1.07	14.02	-24.66	32.52	14.02	53.46	3.47	1.50	5.70
LV77	LV77-14	174.79	72.24	1.25	25.27	-24.48	28.70	25.27	46.03	3.58	3.15	5.73
LV77	LV77-15	170.89	71.25	1.27	54.00	-24.97	5.30	54.00	40.70	0.67	6.87	5.18
LV77	LV77-16	166.04	70.08	0.45	5.07	-25.50	25.67	5.07	69.26	1.16	0.23	3.13
LV77	LV77-17	166.22	71.01	0.26	0.00	-25.67	26.21	0.00	73.79	0.67	0.00	1.89
LV77	LV77-18	166.54	71.67	0.65	5.81	-25.66	23.02	5.81	71.17	1.49	0.38	4.60
LV77	LV77-19	162.63	72.15	0.33	4.60	-25.55	25.17	4.60	70.23	0.84	0.15	2.34
LV77	LV77-20	166.87	72.90	1.07	6.99	-25.51	24.46	6.99	68.55	2.63	0.75	7.36
LV77	LV77-21	167.49	74.13	0.88	20.53	-24.29	34.13	20.53	45.34	3.02	1.82	4.01
LV77	LV77-22	167.83	75.18	0.96	20.60	-23.78	41.34	20.60	38.06	3.96	1.97	3.65
LV77	LV77-23	168.10	75.85	0.96	4.67	-23.00	61.63	4.67	33.70	5.89	0.45	3.22
LV77	LV77-24	168.51	76.60	0.62	21.40	-22.94	52.91	21.40	25.69	3.27	1.32	1.59
LV77	LV77-25	169.25	77.81	0.51	33.17	-22.81	48.02	33.17	18.81	2.43	1.68	0.95
LV77	LV77-26	169.55	78.49	0.57	13.63	-23.81	44.93	13.63	41.44	2.54	0.77	2.34
LV77	LV77-27	169.76	79.15	1.63	0.00	-23.05	63.59	0.00	36.41	10.34	0.00	5.92
LV77	LV77-28	163.49	79.19	0.41	15.90	-23.23	51.99	15.90	32.11	2.16	0.66	1.33
LV77	LV77-29	163.28	78.85	0.66	18.82	-23.07	52.50	18.82	28.68	3.44	1.23	1.88
LV77	LV77-30	162.05	77.90	0.62	16.17	-23.08	53.85	16.17	29.98	3.34	1.00	1.86
LV77	LV77-31	161.31	77.24	0.32	33.09	-23.47	38.66	33.09	28.25	1.22	1.04	0.89
LV77	LV77-32	160.25	76.50	0.80	52.33	-23.65	25.11	52.33	22.56	2.02	4.21	1.81
LV77	LV77-33	159.26	75.85	0.94	52.12	-25.20	3.09	52.12	44.79	0.29	4.89	4.20
LV77	LV77-34	158.50	75.25	0.77	52.05	-25.31	1.56	52.05	46.39	0.12	4.03	3.59
LV77	LV77-35	157.42	74.64	0.88	37.10	-25.51	7.29	37.10	55.61	0.64	3.27	4.90
LV77	LV77-36	155.65	74.10	0.92	12.84	-25.46	21.86	12.84	65.30	2.00	1.18	5.98
LV77	LV77-38	159.77	72.56	0.68	9.56	-26.00	15.99	9.56	74.45	1.09	0.65	5.05
LV77	LV77-39	157.34	72.87	0.37	18.75	-25.51	17.71	18.75	63.54	0.65	0.69	2.33
LV77	LV77-40	153.25	71.90	0.96	0.93	-26.40	15.18	0.93	83.89	1.46	0.09	8.08
LV77	LV77-41	154.13	72.55	0.75	2.02	-27.12	4.35	2.02	93.63	0.33	0.15	7.05

Cruise	Station	Longitude	Latitude	TOC (%)	H-Print (%)	$\delta^{13}\text{C}_{\text{org}}$ (‰)	$f_{\text{sym}}$ (%)	$f_{\text{pela}}$ (%)	$f_{\text{terr}}$ (%)	$\text{OC}_{\text{sym}}$ ( $\text{mg g}^{-1}$ d. w.)	$\text{OC}_{\text{pela}}$ ( $\text{mg g}^{-1}$ d. w.)	$\text{OC}_{\text{terr}}$ ( $\text{mg g}^{-1}$ d. w.)
LV77	LV77-42	155.19	73.16	1.22	4.95	-25.77	21.94	4.95	73.11	2.67	0.60	8.88
LV77	LV77-43	153.16	73.37	0.78	0.91	-25.45	28.77	0.91	70.32	2.23	0.07	5.45
LV77	LV77-44	151.19	73.54	0.60	2.21	-25.39	28.85	2.21	68.94	1.72	0.13	4.10
LV77	LV77-45	148.50	73.70	0.69	1.56	-26.18	17.97	1.56	80.47	1.24	0.11	5.54
ARC11	20Z4	-166.61	73.54	1.78	20.31	-22.89	54.25	20.31	25.44	9.63	3.61	4.52
ARC11	20Z3	-167.16	74.34	0.78	20.85	-22.52	59.24	20.85	19.91	4.64	1.63	1.56
ARC11	20P1-6	-166.62	75.44	0.69	48.04	-23.13	34.98	48.04	16.98	2.40	3.30	1.16
ARC11	20P2-5	-163.68	76.60	0.87	9.09	-22.73	62.99	9.09	27.92	5.45	0.79	2.42
ARC11	20E2	179.99	75.84	0.57	0.00	-22.99	64.44	0.00	35.56	3.66	0.00	2.02
ARC11	20E1	-179.89	75.01	1.23	5.70	-23.72	50.73	5.70	43.57	6.25	0.70	5.37
ARC11	20R2	-168.92	75.61	0.96	31.02	-22.64	51.70	31.02	17.28	4.96	2.97	1.66
ARC11	20R1	-169.13	74.64	0.76	9.51	-22.02	72.85	9.51	17.64	5.53	0.72	1.34
ARC11	20R5	-168.94	77.76	1.18	0.00	-23.54	56.63	0.00	43.37	6.66	0.00	5.10
ARC06	14R14	-160.43	78.63	0.45	0.00	-23.10	62.86	0.00	37.14	2.83	0.00	1.67
ARC06	14R12	-163.89	77.00	0.50	0.00	-22.70	68.57	0.00	31.43	3.43	0.00	1.57
ARC06	14R11	-166.20	76.15	0.79	0.00	-21.60	84.29	0.00	15.71	6.66	0.00	1.24
ARC06	14R10	-167.90	75.43	0.56	0.00	-23.80	52.86	0.00	47.14	2.96	0.00	2.64
ARC06	14R09	-169.03	74.61	1.33	6.90	-21.90	76.06	6.90	17.04	10.12	0.92	2.27
ARC06	14R08	-169.00	74.00	1.27	4.49	-22.30	71.72	4.49	23.79	9.11	0.57	3.02
ARC06	14R07	-168.97	73.00	1.47	2.34	-22.00	77.23	2.34	20.43	11.35	0.34	3.00
ARC06	14R03	-169.05	68.62	1.11	13.33	-22.70	60.95	13.33	25.72	6.77	1.48	2.85
ARC06	14S03	-157.08	72.24	1.75	19.24	-22.80	56.15	19.24	24.61	9.83	3.37	4.31
ARC06	14S02	-157.46	71.92	1.72	15.58	-22.70	59.67	15.58	24.75	10.26	2.68	4.26
ARC06	14S01	-157.93	71.62	1.07	1.67	-22.80	66.19	1.67	32.14	7.08	0.18	3.44
ARC06	14C04	-166.99	71.01	1.28	4.94	-20.90	91.46	4.94	3.60	11.71	0.63	0.46
ARC06	14C01	-168.14	69.22	0.89	11.11	-23.60	49.37	11.11	39.52	4.39	0.99	3.52
ARC06	14C03	-166.48	69.03	1.06	2.90	-24.40	42.63	2.90	54.47	4.52	0.31	5.77
ARC06	14C13-5	-159.18	75.20	0.75	0.00	-22.60	70.00	0.00	30.00	5.25	0.00	2.25
ARC06	14CC6	-167.13	68.24	0.60	18.31	-24.00	39.54	18.31	42.15	2.37	1.10	2.53
ARC06	14CC4	-167.51	68.13	0.58	19.30	-23.50	46.11	19.30	34.59	2.67	1.12	2.01
ARC06	14CC3	-167.90	68.10	0.38	12.50	-22.90	58.57	12.50	28.93	2.23	0.48	1.10
ARC06	14CC2	-168.24	67.90	0.53	15.56	-23.20	52.54	15.56	31.90	2.78	0.82	1.69
ARC03	08R15	-169.01	73.99	1.18	0.00	-24.76	39.14	0.00	60.86	4.62	0.00	7.18
ARC03	08R11	-168.98	72.00	1.71	0.00	-22.94	65.14	0.00	34.86	11.14	0.00	5.96
ARC03	08R09	-168.97	70.99	1.33	6.90	-23.43	54.20	6.90	38.90	7.21	0.92	5.17
ARC03	08R03	-169.02	68.00	1.68	18.18	-22.71	58.04	18.18	23.78	9.75	3.05	4.00
ARC03	08R01	-169.00	67.00	0.73	17.50	-23.86	42.00	17.50	40.50	3.07	1.28	2.96
ARC03	08M07	-171.99	75.01	1.11	0.00	-22.64	69.43	0.00	30.57	7.71	0.00	3.39
ARC03	08S14	-157.92	73.17	1.27	0.00	-23.87	51.86	0.00	48.14	6.59	0.00	6.11
ARC03	08B11	-165.03	75.00	1.18	0.00	-23.60	55.71	0.00	44.29	6.57	0.00	5.23
ARC03	08C33	-167.51	68.92	1.17	4.00	-24.15	45.57	4.00	50.43	5.33	0.47	5.90

Cruise	Station	Longitude	Latitude	TOC (%)	H- Print (%)	$\delta^{13}\text{C}_{\text{org}}$ (‰)	$f_{\text{sym}}$ (%)	$f_{\text{pela}}$ (%)	$f_{\text{terr}}$ (%)	$\text{OC}_{\text{sym}}$ (mg g <sup>-1</sup> d. w.)	$\text{OC}_{\text{pela}}$ (mg g <sup>-1</sup> d. w.)	$\text{OC}_{\text{terr}}$ (mg g <sup>-1</sup> d. w.)
ARC03	08C35	-166.51	68.92	1.55	3.64	-24.79	36.63	3.64	59.73	5.68	0.56	9.26
ARC03	08C13	-166.75	71.80	1.45	5.89	-23.40	55.21	5.89	38.90	8.01	0.85	5.64
ARC03	08C17	-161.98	71.49	1.49	2.58	-24.18	45.95	2.58	51.47	6.85	0.38	7.67
ARC03	08C19	-159.98	71.45	1.19	2.09	-23.77	52.09	2.09	45.82	6.20	0.25	5.45

## References

Bai, Y., Sicre, M.-A., Ren, J., Jalali, B., Klein, V., Li, H., Lin, L., Ji, Z., Su, L., Zhu, Q., Jin, H. and Chen, J.: Centennial-scale variability of sea-ice cover in the Chukchi Sea since AD 1850 based on biomarker reconstruction, *Environ. Res. Lett.*, 17, 4, <https://doi.org/10.1088/1748-9326/ac5f92>, 2022.

Kim, J. -H., Gal, J. -K., Jun, S. -Y., Smik, L., Kim, D., Belt, S. T., Park, K., Shin, K. -H. and Nam, S. -I.: Reconstructing spring sea ice concentration in the Chukchi Sea over recent centuries: insights into the application of the PIP<sub>25</sub> index, *Environ. Res. Lett.*, 14(12), 125004, <https://doi.org/10.1088/1748-9326/ab4b6e>, 2019.

Smik, L., Cabedo-Sanz, P. and Belt, S. T.: Semi-quantitative estimates of paleo Arctic sea ice concentration based on source-specific highly branched isoprenoid alkenes: a further development of the PIP<sub>25</sub> index, *Org. Geochem.*, 92, 63-69, <https://doi.org/10.1016/j.orggeochem.2015.12.007>, 2016.

Walsh, J. E., Fetterer, F., Scott Stewart, J. and Chapman, W. L.: A database for depicting Arctic sea ice variations back to 1850, *Geogr. Rev.*, 107(1), 89-107, <https://doi.org/10.1111/j.1931-0846.2016.12195.x>, 2017.

Xiao, X., Fahl, K., Müller, J. and Stein, R.: Sea-ice distribution in the modern Arctic Ocean: Biomarker records from trans-Arctic Ocean surface sediments, *Geochim. Cosmochim. Acta*, 155, 16-29, <https://doi.org/10.1016/j.gca.2015.01.029>, 2015a.